

Expanded View Figures

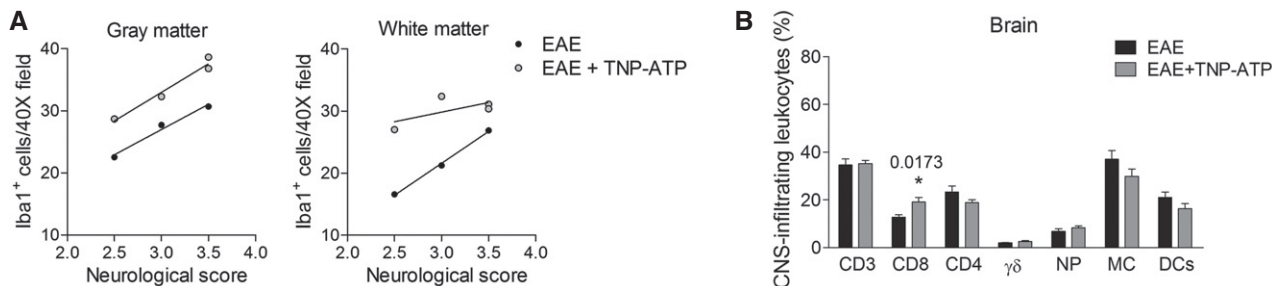


Figure EV1. Immune cell analysis in EAE and TNP-ATP-treated EAE mice.

- A Correlation between the neurological score and the number of Iba1⁺ cells in gray matter and white matter of the spinal cord.
- B Flow cytometric quantification of immune cell infiltrates (gating as in Fig 2E) in the brain of TNP-ATP-treated or non-treated mice analyzed at the peak of symptoms after EAE induction ($n = 8$). Data are presented as mean \pm s.e.m. and were analyzed by Student's *t*-test. * $P < 0.05$.

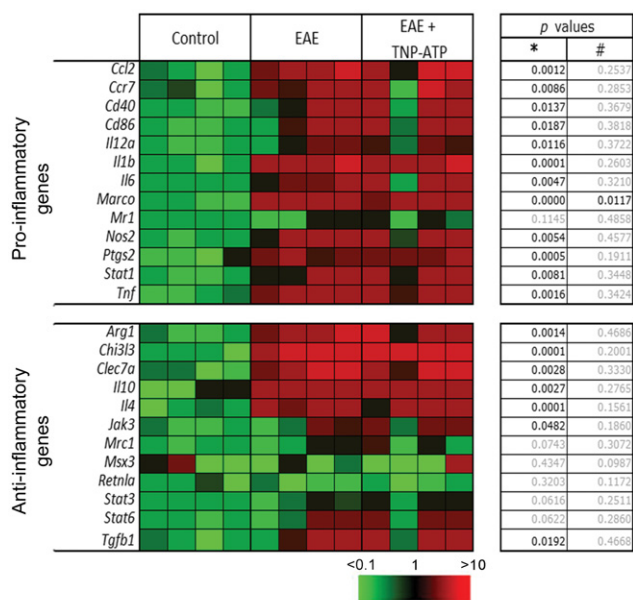


Figure EV2. Heatmap of pro-inflammatory and anti-inflammatory genes at EAE peak.

Expression of most pro-inflammatory genes and some anti-inflammatory genes was increased in the spinal cord of EAE mice ($n = 3$) at the peak phase, but TNP-ATP did not induce significant changes ($n = 3$). Tables indicate statistical significance between control and EAE (*) and between EAE and EAE + TNP-ATP (#). Statistics were performed with Student's *t*-test.

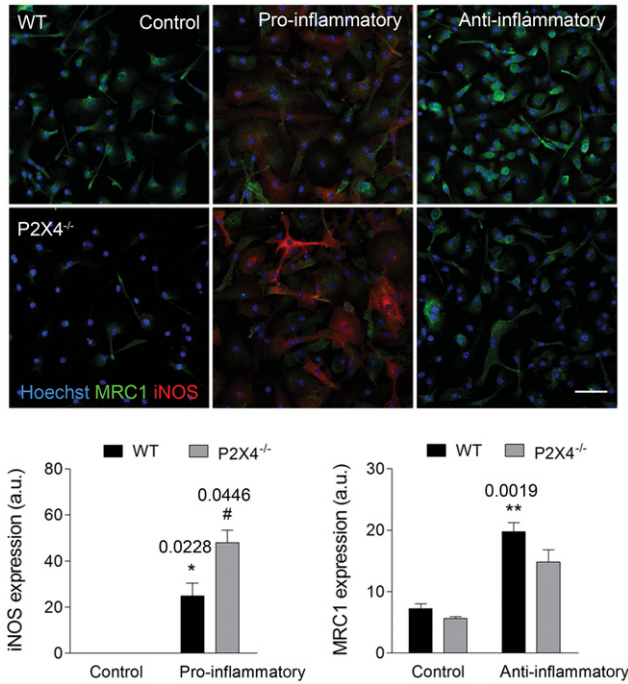


Figure EV3. Pro-inflammatory and anti-inflammatory polarization in wild-type and P2X4^{-/-} microglia.

Staining for iNOS (red) and mannose receptor (MRC1, green) in control, pro-inflammatory, and anti-inflammatory microglia from wild-type and P2X4^{-/-} mice. Scale bar = 50 μ m ($n = 4$ experiments performed in triplicate). Data are presented as mean \pm s.e.m. and were analyzed by Student's t -test. *[#] $P < 0.05$, ** $P < 0.01$. Symbols indicate significance versus control (*) or versus pro-/anti-inflammatory microglia ([#]).

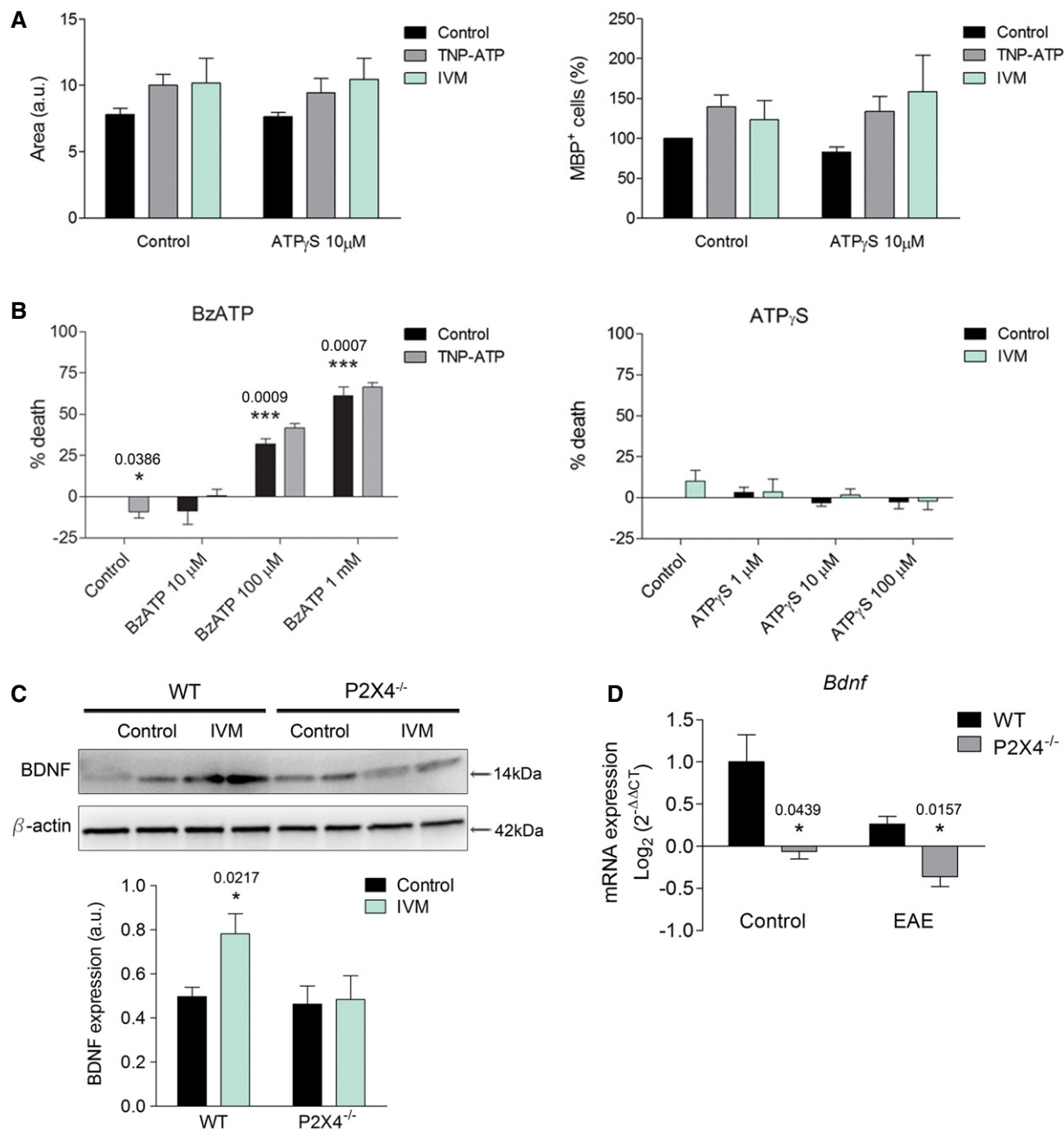


Figure EV4. Functional role of P2X4R in oligodendrocytes in vitro.

A Effect of ATP_{7S} (10 μ M) \pm ivermectin or TNP-ATP (10 μ M) on oligodendrocyte differentiation quantified on the basis of the number of MBP⁺ cells/total cell number and the area of the cells. Area was calculated with ImageJ software ($n = 3$).

B Oligodendrocyte cell viability after 24-h incubation with BzATP, a broad-spectrum agonist of purinergic receptors, in the absence or presence of TNP-ATP (10 μ M) (left) or ATP_{7S} (right) in the absence or presence of IVM (3 μ M) ($n = 3$).

C Western blot analysis of BDNF in control and IVM-treated wild-type and P2X4^{-/-} microglia ($n = 3$).

D *Bdnf* mRNA levels in the spinal cord of WT and P2X4^{-/-} mice in control and after EAE induction ($n = 4$ mice/group).

Data information: Data are presented as mean \pm s.e.m. and were analyzed by one-way ANOVA (B) and Student's *t*-test (C, D). * $P < 0.05$, *** $P < 0.001$.

Source data are available online for this figure.

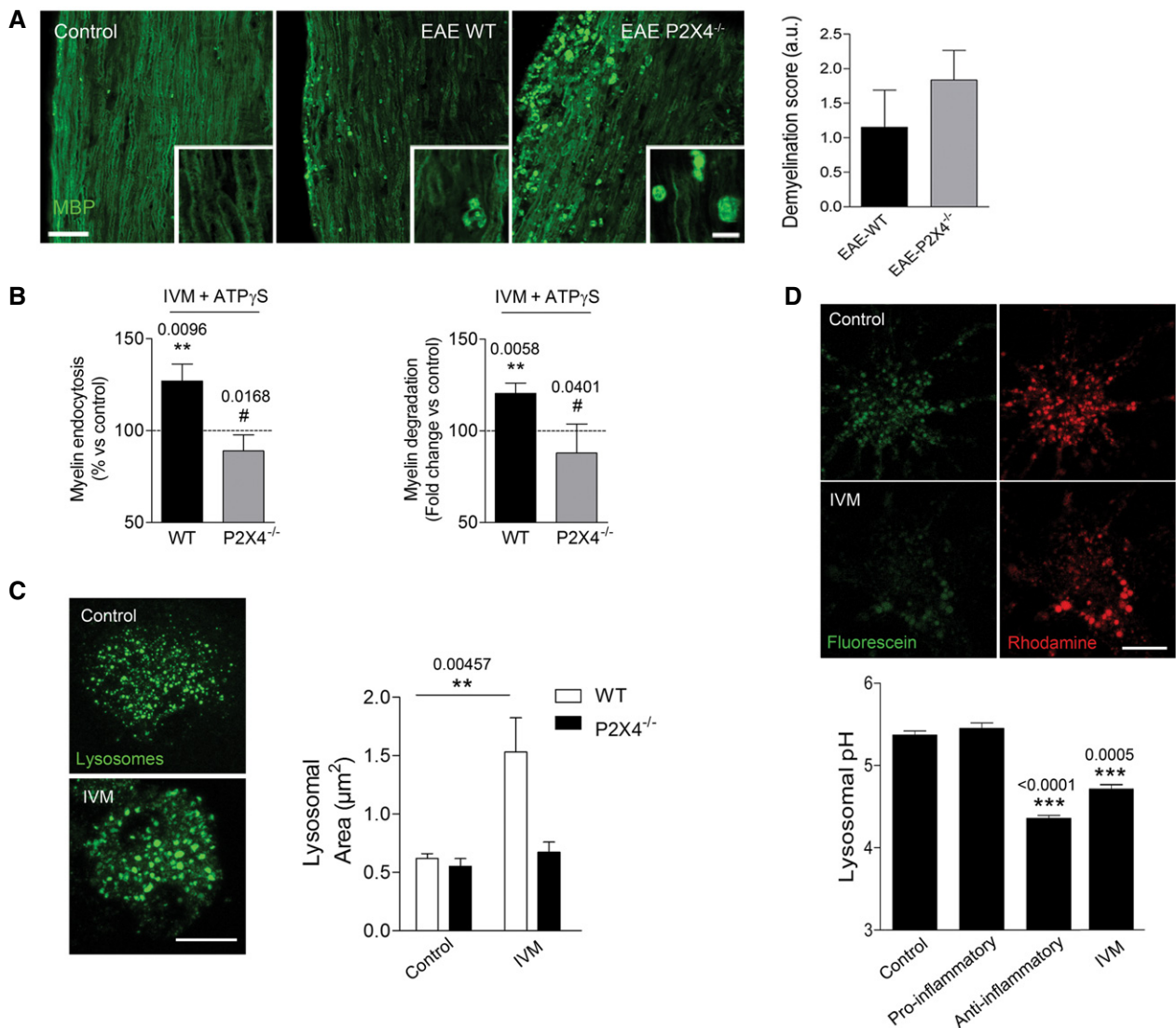


Figure EV5. Role of P2X4R in myelin phagocytosis and lysosome function.

A Spinal cord sections of wild-type ($n = 6$) and P2X4^{-/-} mice ($n = 7$) 35 days after EAE induction stained for MBP. Scale bar = 50 and 10 (inset) μm. Inset images come from different fields at higher magnification. Right, demyelination score analyzed in MBP-stained sections.

B Effect of IVM (3 μM) on myelin endocytosis (1 h) and degradation (3 days) in microglia from wild-type and P2X4^{-/-} mice ($n = 3$).

C Treatment with IVM (3 μM; 16 h) increased late endosome–lysosome (LEL) size in microglia from wild-type and P2X4^{-/-} mice. Representative images and histogram for LEL size distributions under the conditions indicated ($n = 20$ cells from two independent experiments). Scale bar = 10 μm.

D IVM-treated microglia (3 μM) and anti-inflammatory microglia showed an acidic shift in lysosomal pH, as analyzed on the basis of fluorescein/rhodamine–dextran ratio ($n = 20$ cells from two independent experiments). Scale bar = 10 μm.

Data information: Data are presented as mean ± s.e.m. and were analyzed by one-way ANOVA. # $P < 0.05$, ** $P < 0.01$, *** $P < 0.001$. Symbols indicate significance versus control (*) or versus pro-inflammatory microglia (#).